Galactose-Depleted Xyloglucan is Dysfunctional and Leads to Dwarfism in Arabidopsis

Yingzhen Kong, Maria J. Peña, Luciana Renna, Utku Avci, Sivakumar Pattathil, Sami T. Tuomivaara, Xuemei Li, Wolf-Dieter Reiter, Federica Brandizzi, Michael G. Hahn, Alan G. Darvill, William S. York, and Malcolm A. O'Neill

SUPPORTING INFORMATION

Figure S1. RT-PCR analysis of gene transcripts in the mutant lines.

Figure S2. The MALDI-TOF mass spectra and HPAE-PAD profiles of the XyGOs generated by XEG treatment of the 4 N KOH soluble materials from Col-O, *mur3-1*, *mur3-2*, and *mur3-3* mutant plants.

Figure S3. The MALDI-TOF mass spectra and HPAE-PAD profiles of the XyGOs generated by XEG treatment of the 4 N KOH soluble materials from Col-O, *mur3*, *xxt*, and *mur3 xxt* mutant plants.

Figure S4. The phenotypes and MALDI-TOF mass spectra of the XyGOs generated by XEG treatment of the 4 N KOH soluble materials from individual *35Spro MUR3:mur3*, *mur3-1*, and *mur3-2* plants.

Figure S5. The MALDI-TOF mass spectra of the XyGOs released by XEG treatment of Col-O, *mur3-1, mur3-2*, and *mur3-3* AIR.

Figure S6. The effect of the absence of light on hypocotyls length of seedlings carrying single or combine mutations in genes encoding xylosyltransferases XXT1, XXT2, and XXT5 and galactosyltransferases MUR3 and XLT2.

Figure S7. RT-PCR analyses of *XLT2* transcripts in the rossette leaves of *mur3-3*:35Spro:*XLT2* plants.

Figure S8. Intracellular accumulation of cell wall polysaccharides in *mur3* hypocotyls.

Figure S9. The MALDI-TOF mass spectra and HPAE-PAD profiles of the XyGOs generated by XEG treatment of the 4 N KOH soluble materials from Col-O and selected mutant plants grown at 19 ºC and 28ºC.

Figure S10. The effects of temperature on the growth and development of *mur3-3* plants.

Figure S11. Abundance of tandemly repeated XXXG domains in the xyloglucan from transgenic plants.

Table S1. Sidechain compositions of the xyloglucans isolated from the cell walls of Arabidopsis wild-type, *mur3-1*, *mur3-2*, and *mur3-3* plants.

Table S2. The amounts and subunit compositions of the xyloglucan present in the leaf cell walls of wild type and selected *xxt* Arabidopsis mutants.

Table S3. Primers used in this study.

Table S4. Monoclonal antibodies used for glycome profiling.

Protocol S1. Calculating the fraction of a polysaccharide that is composed of domains containing *n* or more tandemly repeated copies of a sequence.

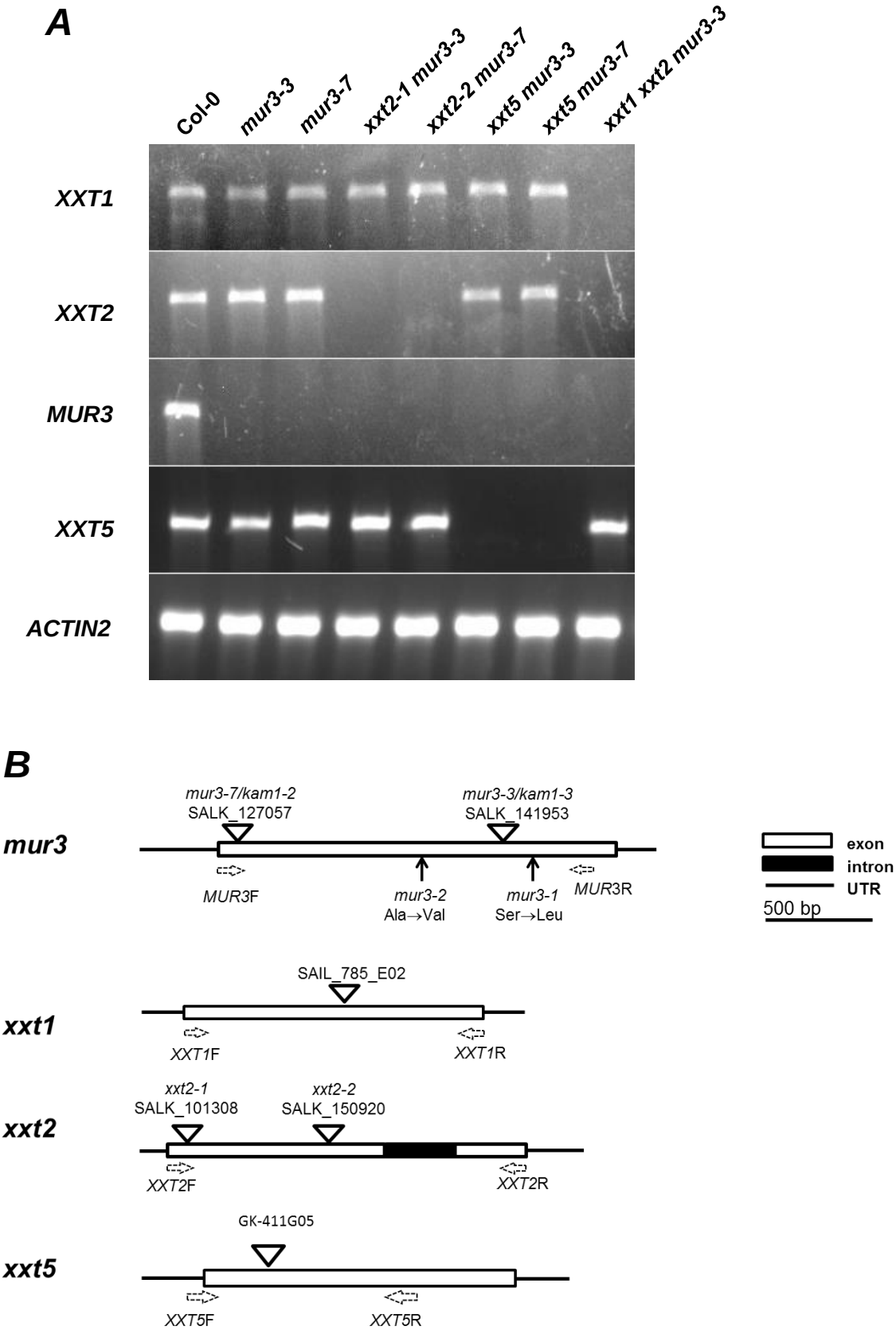

Supplemental Figure S1. RT-PCR analysis of gene transcripts in the mutant lines. A, RT-PCR analysis of gene transcripts in the rosette leaves of the mutant lines. Total RNA (2 µg) was used for reverse transcription in a 20-µL RT-PCR reaction. A portion (0.2 µL) of the reverse transcription products was then used in a 20-µL PCR reaction. Thirty cycles of PCR were used. Primers used are listed in Table S4. B, Location of the T-DNA insertions in the *mur3* and the *xxt1*, *xxt2*, and *xxt5* mutants.

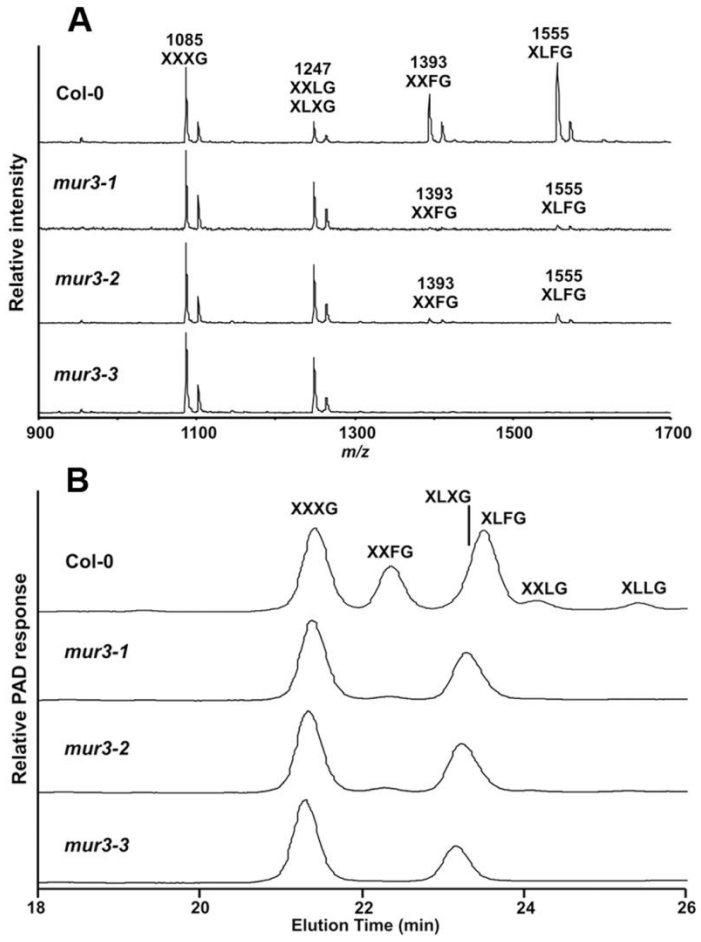

Supplemental Figure S2. The MALDI-TOF mass spectra and HPAE-PAD profiles of the XyGOs generated by XEG treatment of the 4 N KOH soluble materials from Col-O, *mur3-1*, *mur3-2*, and *mur3-3* mutant plants. A, The MALDI-TOF mass spectra of the xyloglucan oligosaccharides. B, The HPAE-PAD profiles of the xyloglucan oligosaccharides. XLXG elutes slightly before XLFG, but these subunits could not be separated.

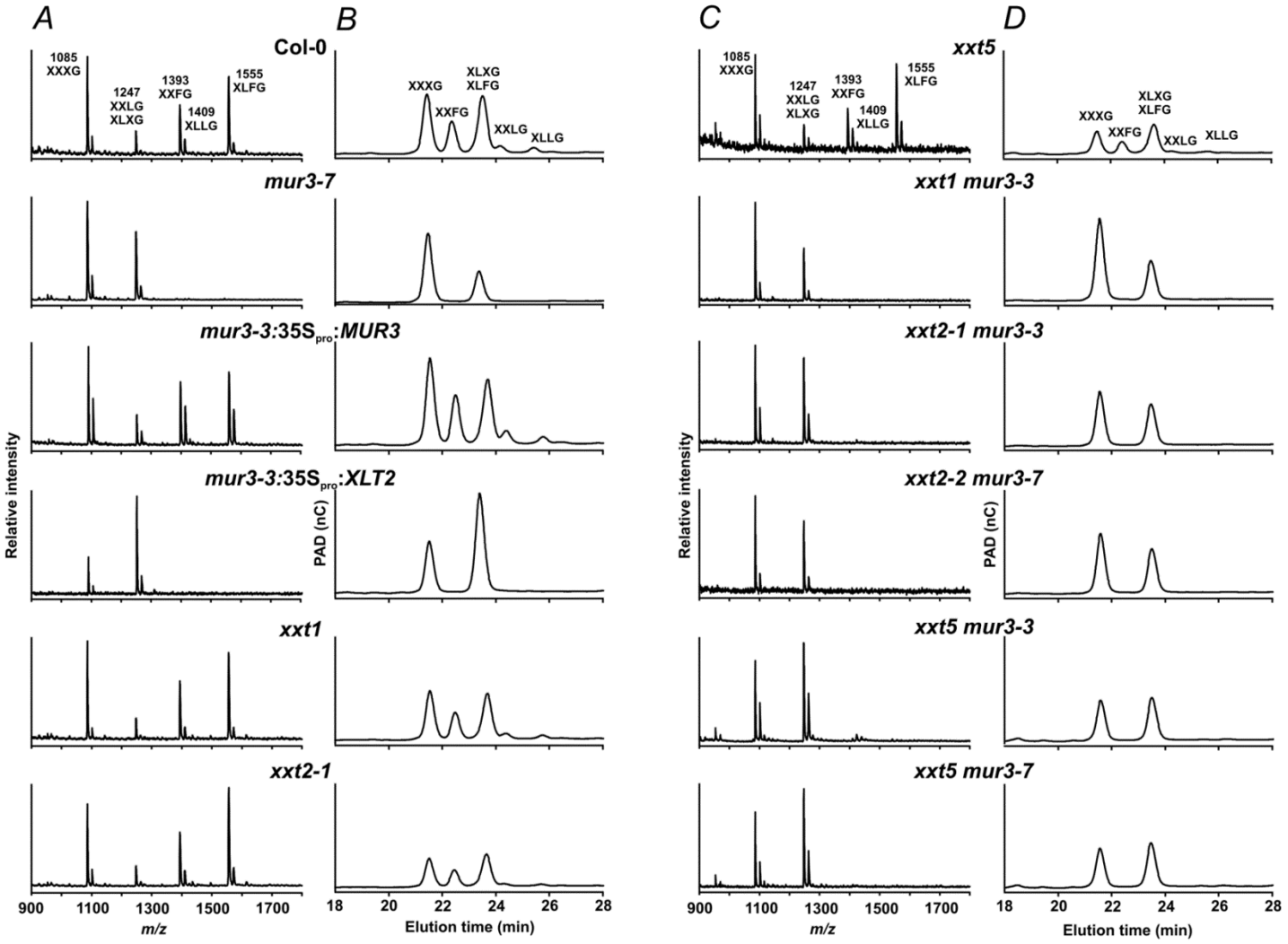

Supplemental Figure S3. The MALDI-TOF mass spectra and HPAE-PAD profiles of the XyGOs generated by XEG treatment of the 4 N KOH soluble materials from Col-O, *mur3*, *xxt*, and *mur3 xxt* mutant plants. A and C, The MALDI-TOF mass spectra of the XyGOs. B and D, The HPAE-PAD profiles of the XyGOs.

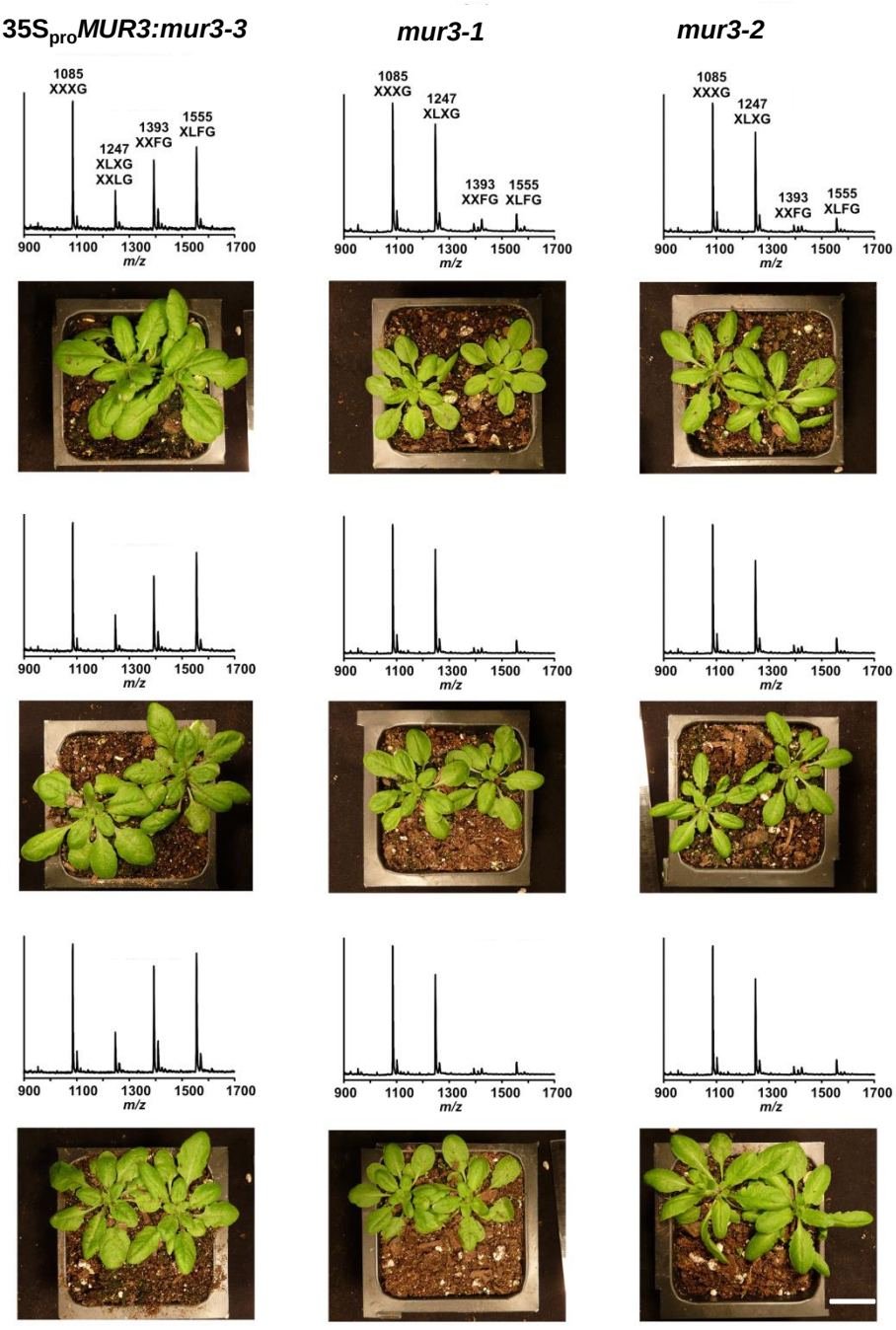

Supplemental Figure S4. The phenotypes and MALDI-TOF mass spectra of the XyGOs generated by XEG treatment of the 4 N KOH soluble materials from individual *35Spro MUR3:mur3*, *mur3-1*, and *mur3-2* plants. Each plant in a pot was separately analyzed but only one mass spectrum is shown. Scal bar = 2.5 cm

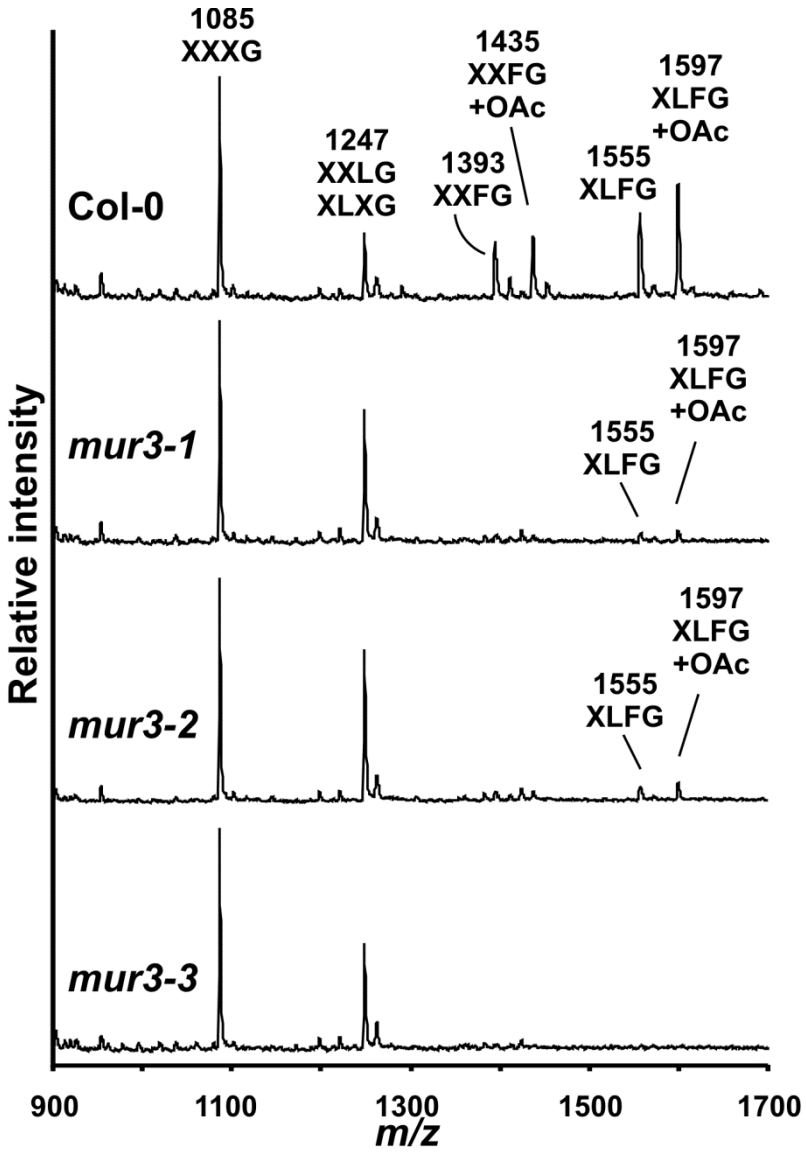

Supplemental Figure S5. The MALDI-TOF mass spectra of the XyGOs released by XEG treatment of Col-O, *mur3-1, mur3-2*, and *mur3-3* AIR.

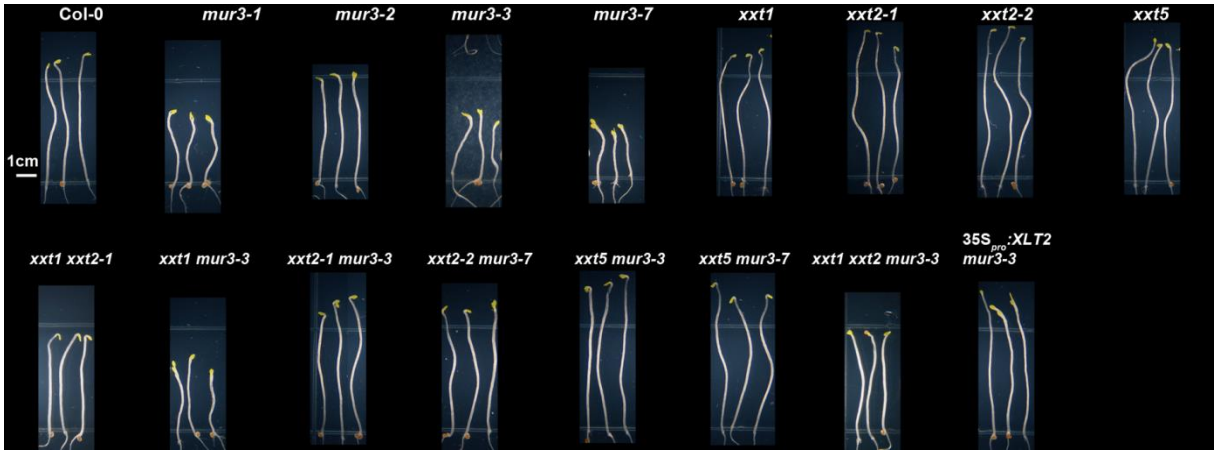

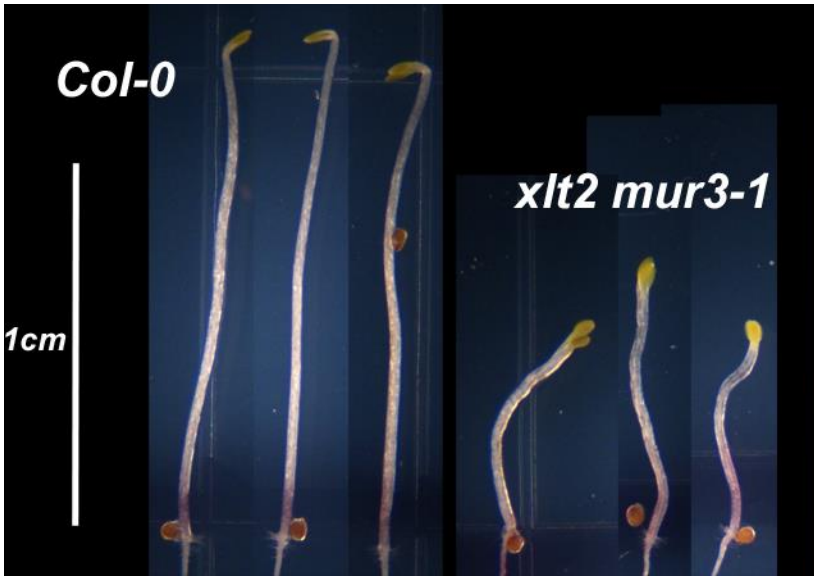

Supplemental Figure S6. The effect of the absence of light on the hypocotyl length of seedlings carrying single or combined mutations in genes encoding xylosyltransferases XXT1, XXT2, and XXT5 and galactosyltransferases MUR3 and XLT2. Col-0 and mutant seeds were stratified for 48 h at 4ºC. The seeds were then germinated and grown for 5 d at 20˚C in the absence of light.

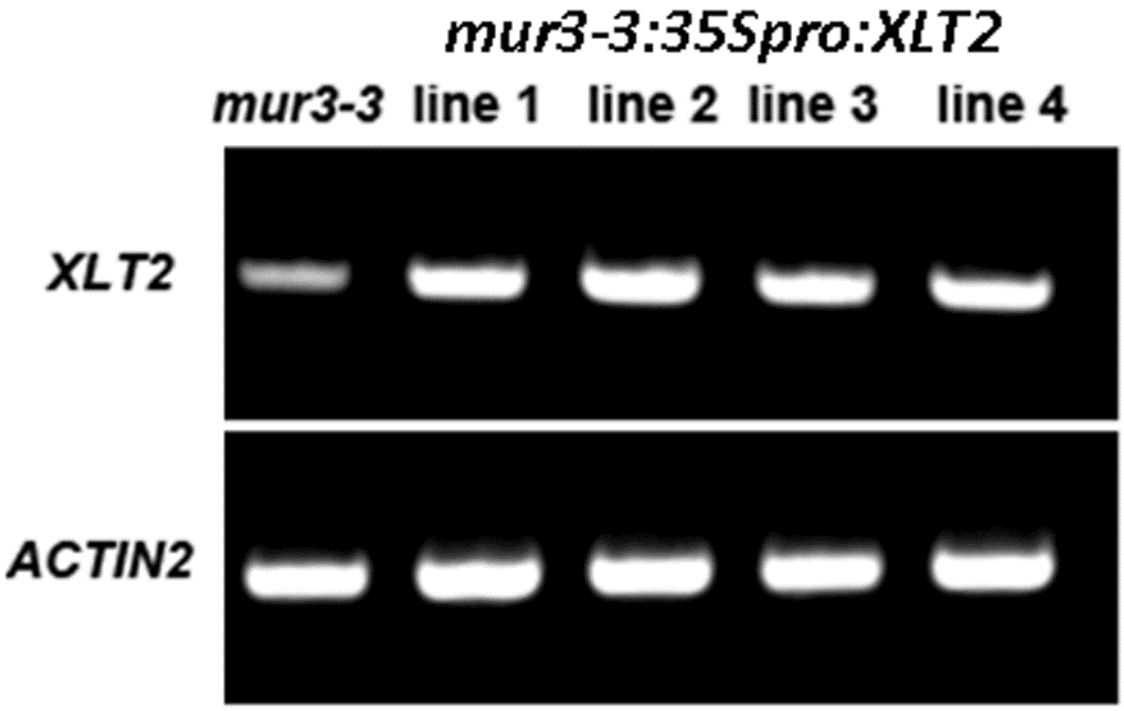

Supplemental Figure S7. RT-PCR analyses of *XLT2* transcripts in the rossette leaves of *mur3-3*:35Spro:*XLT2* plants. Total RNA (2 µg) was used for reverse transcription in a 20 µL RT-PCR reaction. A portion (0.2 µL) of the reverse transcription products was then used in a 20 µL PCR reaction. Thirty cycles of PCR were used. Four independent *mur3-3*:35Spro:*XLT2* lines were analyzed.

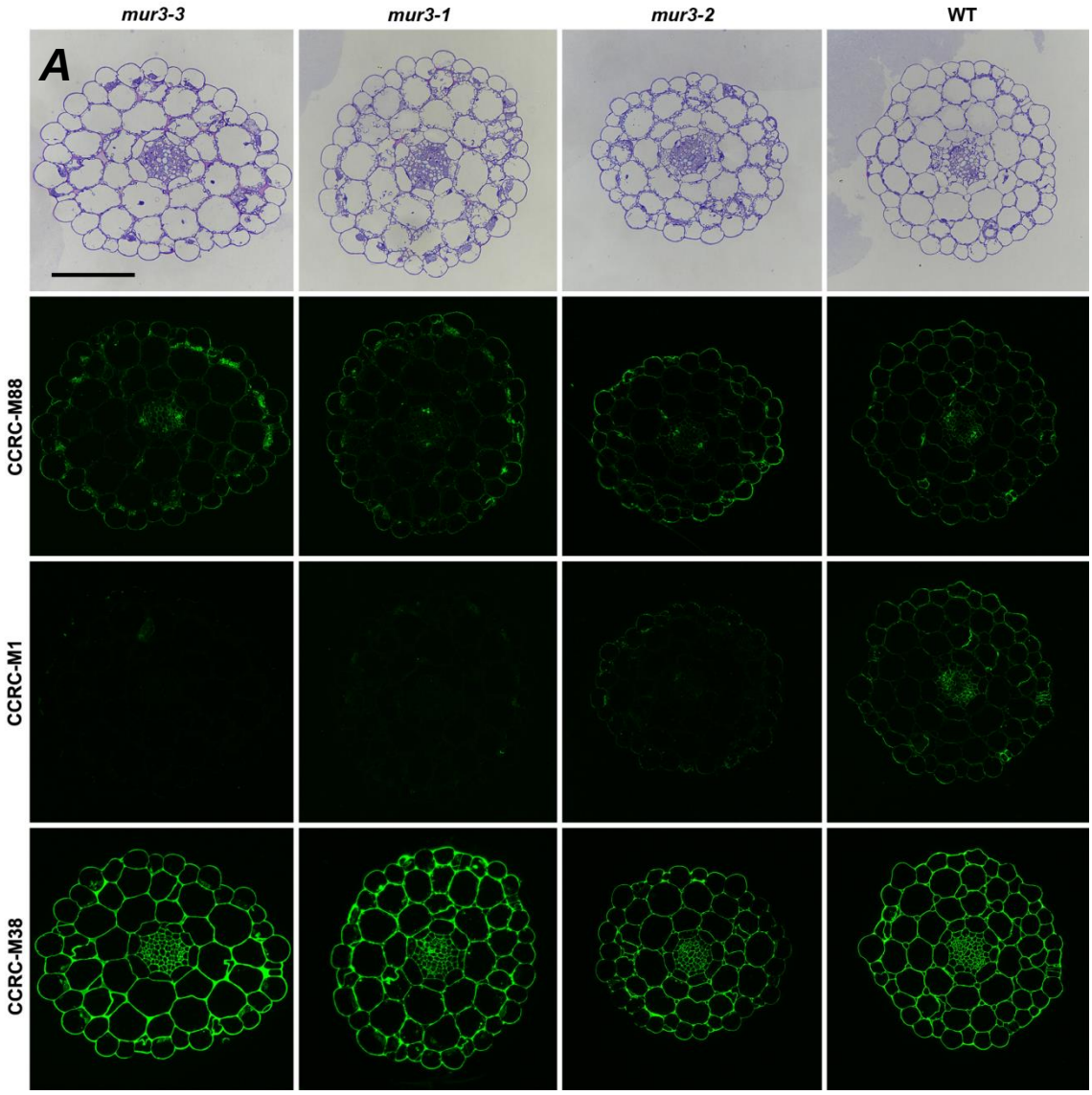

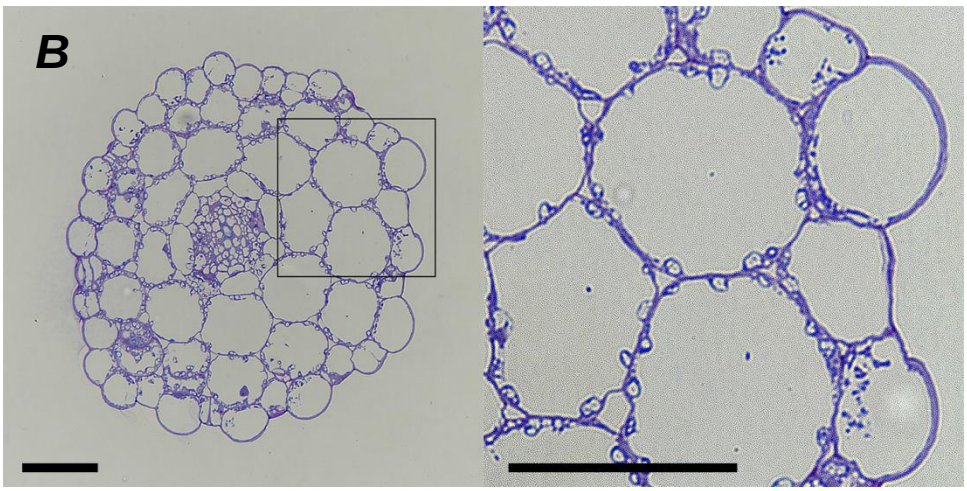

Supplemental Figure S8. Intracellular accumulation of cell wall polysaccharides in *mur3* hypocotyls. A, Images of cross sections of the hypocotyls stained with toluidine or labeled with antibodies that recognize xyloglucan (CCRC-M88), fucosylated xyloglucan (CCRC-M1), and de-esterified homogalacturonan (CCRC-M38). Bar is100μm. B, Cross section of 35SproMUR3:mur3-3 reveals the absence of intracellular aggregates. Bars are 50 μm.

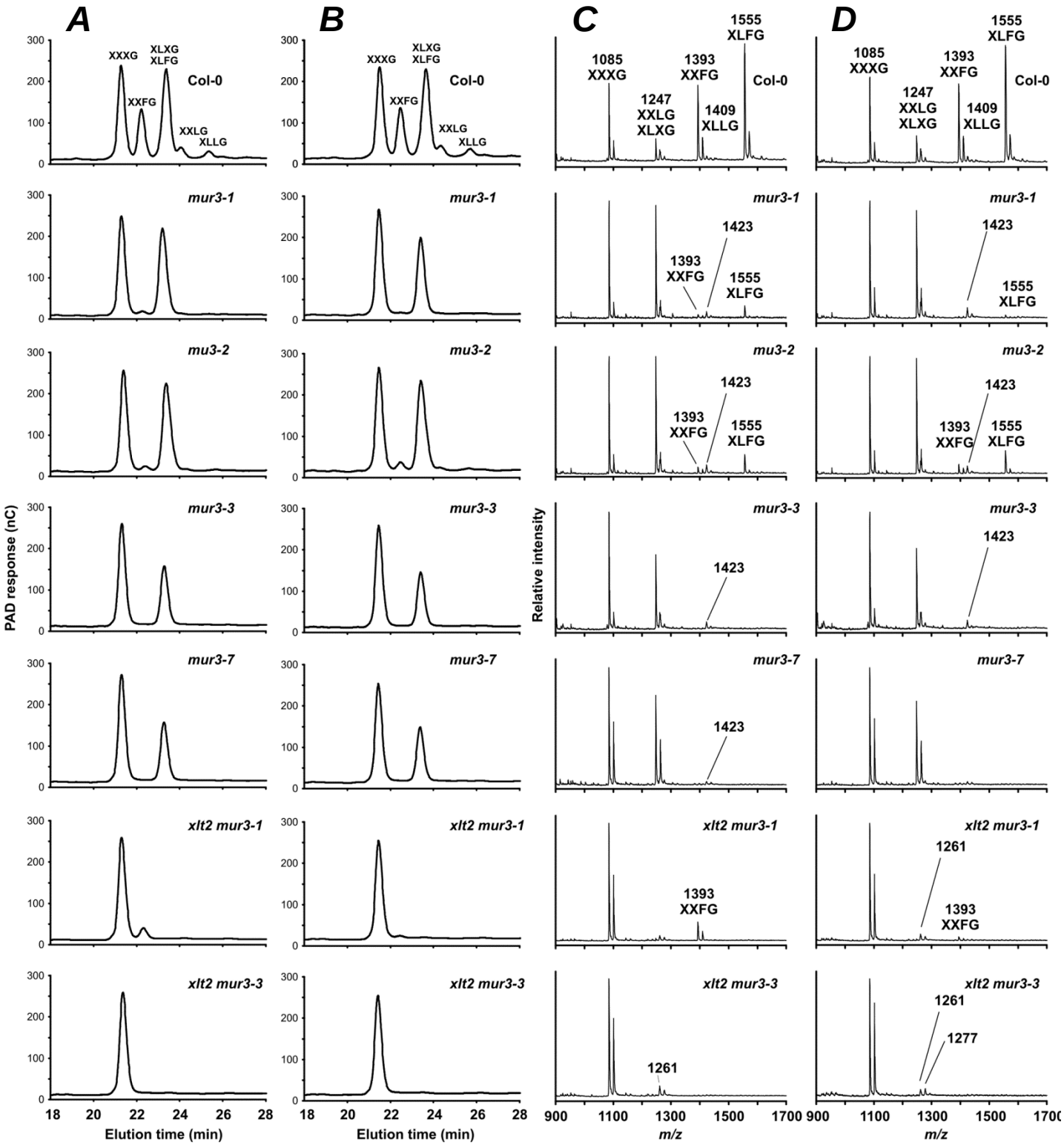

Supplemental Figure S9. The MALDI-TOF mass spectra and HPAE-PAD profiles of the XyGOs generated by XEG treatment of the 4 N KOH soluble materials from Col-O and selected mutant plants grown at 19ºC and 28ºC. A, The HPAE-PAD profiles of the XyGOs generated by XEG treatment of the 4 N KOH soluble materials from plants grown at 19ºC. B, The HPAE-PAD profiles of the XyGOs generated by XEG treatment of the 4 N KOH soluble materials from plants grown at 28ºC. C, The MALDI-TOF mass sepctra of the XyGOs generated by XEG treatment of the 4 N KOH soluble materials from plants grown at 19ºC. D, The MALDI-TOF mass spectra of the XyGOs generated by XEG treatment of the 4 N KOH soluble materials from plants grown at 28ºC. The ions at *m/z* 1423, 1261, and 1277 are from the matrix.

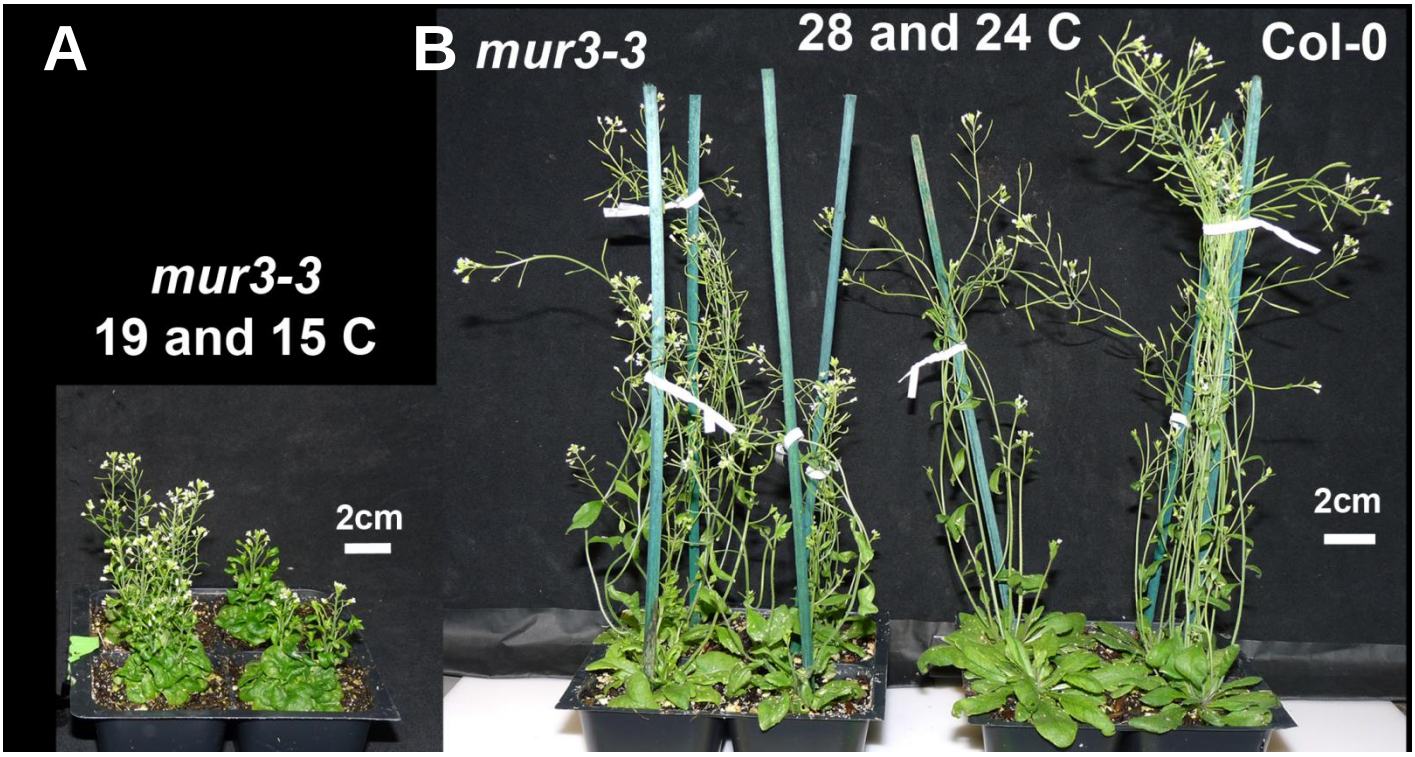

Supplemental Figure S10. The effects of temperature on the growth and development of *mur3-3* plants. A, *mur3-3* plants grown with a 14 h light (19ºC) and 10 h dark (15ºC) cycle, respectively. B, *mur3-3* and Col-0 plants grown with a 14 h light (28ºC) and 10 h dark (24ºC) cycle.

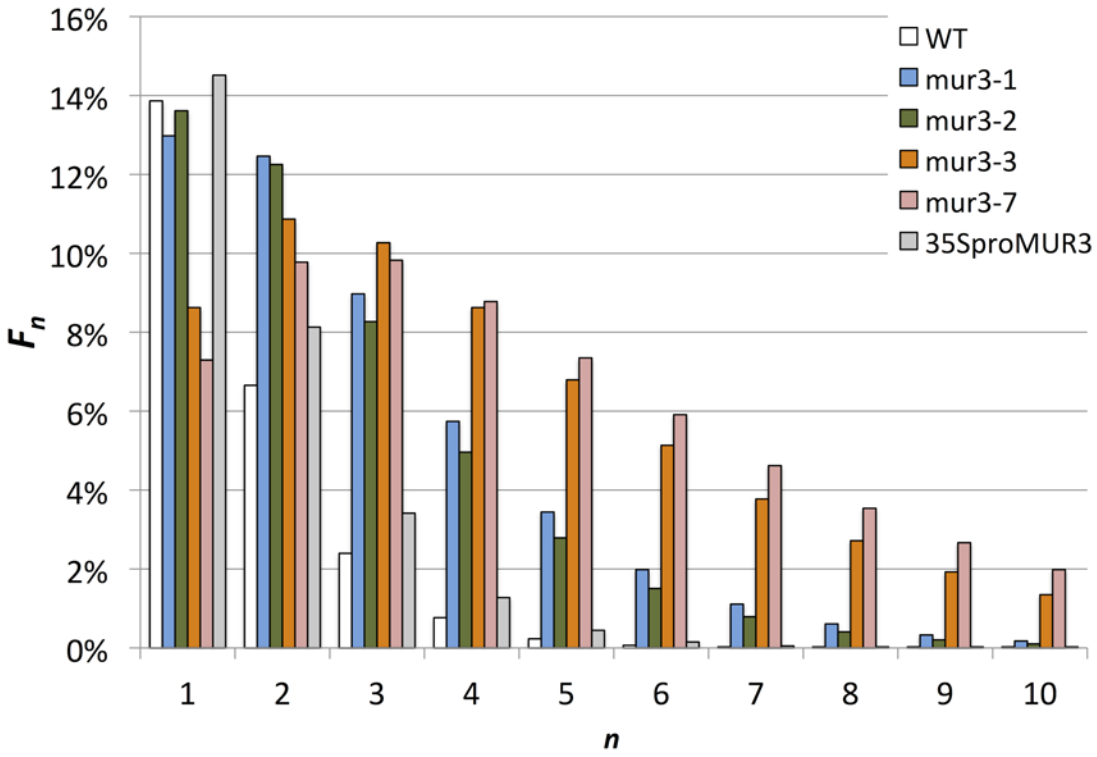

Supplemental Figure S11. Abundance of tandemly repeated XXXG domains in the xyloglucan from transgenic plants. The fraction F_n of each xyloglucan that is composed of domains consisting of exactly *n* tandemly repeated XXXG sequences is plotted as a function of *n*. This shows that domains consisting of 5 or more tandemly repeated XXXG sequences comprise a much higher proportion of the xyloglucan in *mur3-3* and *mur3-7* plants than in xyloglucan from the other plants shown. Our data thus suggests that the dysfunctional properties of the *mur3-3* and *mur3-7* xyloglucan are due to the aggregation or otherwise aberrant interactions of the large tandemly repeated XXXG domains. See Supplemental Protocol S1 for details of the calculations used to generate this figure.

Table S1. Sidechain compositions of the xyloglucans isolated from the cell walls of Arabidopsis wild-type, *mur3-1*, *mur3-2*, and *mur3-3* plants.

Plant	Sidechain distribution ($X_cX_bX_aG$)*				
	Xyl_c	Xyl_{b+a}	$Gal\rightarrow Xyl_b$	$Gal\rightarrow Xyl_a$	$Fuc\rightarrow Gal\rightarrow Xyl_a$
Wild-type	34	39	8	3	15
mur3-1	34	54	11	<1	1
mur3-2	34	51	12	1	2
mur3-3	33	57	9	nd†	nd

*The locations of the sidechains were determined by ^{1}H-NMR spectroscopic analyses of the xyloglucan oligosaccharides generated by XEG treatment of the wild-type and mutant 4 N KOH-soluble xyloglucans. Approximately 30 plants for each line were harvested and pooled for the analyses. The subscript letters indicate the position of the sidechain on the backbone relative to the unsubstituted glucosyl residue (G). The relative proportions of the sidechains were determined by integration of selected anomeric proton resonances in the ^{1}H-NMR spectra. Thus, in wild-type xyloglucan, terminal Xyl at Xyl_c and Xyl_{b+a}accounts for 34% and 39%, respectively, of the sidechains, terminal Gal at Xyl_b and terminal Gal at Xyl_a account for 8% and 3%, respectively, of the sidechains, and 14% of the sidechains are fucosylated. †nd, not detected.

Table S2. The amounts and subunit compositions of the xyloglucan present in the leaf cell walls of wild type and selected *xxt* Arabidopsis mutants.

Genotype*	Xyloglucan (mg/g AIR)†	Xyloglucan subunit composition (%)‡					
		XXXG	XXLG§	XLXG	XXFG	XLLG§	XLFG
Col-0	13 ± 2	25 ± 1	<1	9 ± 1	24 ± 1	<1	42 ± 3
xxt1	11 ± 3	26 ± 2	<1	10 ± 1	22 ± 1	<1	42 ± 2
xxt2-1	8 ± 1	24 ± 1	<1	10 ± 1	20 ± 1	<1	46 ± 1
xxt2-2	8 ± 2	22 ± 2	<1	8 ± 2	22 ± 1	<1	48 ± 1
xxt5	7 ± 1	23 ± 1	<1	11 ± 1	19 ± 1	<1	47 ± 1
xxt1 xxt2-1	nd¶	nd	nd	nd	nd	nd	nd
xxt1 xxt5	5 ± 1	23± 4	<1	10 ± 2	22 ± 1	<1	45 ± 3
xxt2-1 xxt5	3 ± 1	23 ± 1	<1	11 ± 1	22 ± 1	<1	44 ± 1

*All plants have a wild type phenotype (see Fig. 2). †Determined from the amounts of isoprimeverose released by Driselase treatment of the AIR. ‡Determined from the abundance of the $[M + Na]^+$ ions in the MALDI-TOF mass spectra. Xyloglucan oligosaccharides were generated by XEG treatment of the 4 N KOH-soluble materials from at least three individual plants. §The XXLG and XLLG subunits were detected by HPAEC-PAD. ¶nd, not detected. The cell walls of the *xxt1 xxt2* double mutant contain no detectable amounts of xyloglucan.

Table S3. Primers used in this study

Primers used for PCR	5'→ 3'
MUR3-3 LP	TGCAAACGAAATTAAACATAGGC
MUR3-3 RP	GAAGAAGAAACTGATTGGGGC
MUR3-7 LP	CAAGGAAATGATCTTTTCCCC
MUR3-7 RP	ATTGACGGTGATGAAGACCAG
XXT1 LP	TAAACGTGTGTCCCCTAAACG
XXT1 RB	AGAGAAATCTCGAGACCGGAC
SAIL LB1	GCCTTTTCAGAAATGGATAAATAGCCTTGCTTCC
XXT2-1 LP	TAAATTGTTTCCGCGGTACAC
XXT2-1 RP	AGTCACCAAAAGAACACGTGG
XXT2-2 LP	ACAAAGTGAGTCACCAATGGC
XXT2-2 RP	GGAGATTCTTCTTCCGGTGAC
XXT5 LP	GATCATCTGCCTCAAAAGCTG
XXT5 RP	ACAAAGTTGATGGTCGCAAAC
GABI 8760	GGGCTACACTGAATTGGTAGCTC
XLT2 OX F	GGTACCTATGCTTCCTGTCTCAAATCCTTC
XLT2 OX R	TCTAGACCAATCATCATCTCCATTTGTACC
P1300 R	CCAGACAAGTTGGTAATGGTAG
Primers for RT-PCR	
MUR3 F	CCAAGGGTTTCTATGAGGCGTC
MUR3 R	GAAGAACGGGTCCCACACATGG
XXT1 F	ATGATAGAGAAGTCTATAGGAGCGCA
XXT1 R	CGCAAAATTAAAAGATACAAAACAA
XXT2 F	ATGATTGAGAGGTGTTTAGGAGCTTA
XXT2 R	CCTAAACGCAAAACCGATTC
XXT5 F	GATCATCTGCCTCAAAAGCTG
XXT5 R	ACAAAGTTGATGGTCGCAAAC
XLT2 F	TTGGATCCGGAATCAGCTAC
XLT2 R	AATCCACCGTCCGACACTTC
Actin2 F	TGGTCGTACAACCGGTATTGTGC
Actin2 R	TCATACGGTCAGCGATACCTGAG

Table S4. **Monoclonal antibodies used for glycome profiling**

Xyloglucan*	Fucosylated xyloglucan†
CCRC-M54‡	CCRC-M102
CCRC-M48	CCRC-M39
CCRC-M49	CCRC-M106
CCRC-M96	CCRC-M84
CCRC-M50	CCRC-M1
CCRC-M51	
CCRC-M53	
CCRC-M100	
CCRC-M103	
CCRC-M58	
CCRC-M86	
CCRC-M55	
CCRC-M52	
CCRC-M99	
CCRC-M95	
CCRC-M101	
CCRC-M104	
CCRC-M89	
CCRC-M93	
CCRC-M87	
CCRC-M88	
CCRC-M57	
CCRC-M90	

*mAbs bind to xyloglucan irrespective of the presence or absence of fucosylated side chains. †mAbs bind only to xyloglucan that contains fucosylated side chains. ‡For additional information about these antibodies see http://www.wallmabdb.net.

Supplemental Protocol S1

Calculating the Fraction of a Polysaccharide that is composed of Domains Containing *n* or more Tandemly Repeated Copies of a Sequence.

An internal domain consisting of exactly *n* (no more, no less) tandem copies of the sequence **S** (where **S** is a defined subsequence such as XXXG) must have the sequence [NOT **S**] at each end. If the probability of having subsequence **S** at a randomly chosen site in a randomly chosen polymer is *P*, then the probability of a domain [NOT **S**]-$\mathbf{S}_n$-[NOT **S**] starting at that site is calculated by multiplying the probability of *n* + 2 required independent events.

Hence, $P_n = P^n (1 - P)^2$

Note that this does not account for domains at the end of the polymer, which do not contribute significantly to the probability for long polysaccharides.

Domains with exactly *n* tandem copies of **S** constitute a specific fraction F_n of the total sequence of the polymers in the sample. The value of F_n is calculated as the probability P_n of the $\mathbf{S}_n$ domain multiplied by the length *n* (number of tandem repeats) of the sequence. That is,

$$F_n = nP_n = nP^n (1-P)^2$$

As an example, the fractions F_n of the polymer composed of domains with exactly *n* tandemly repeated **S** subsequences for $P = 0.5$ and $P = 0.01$ are shown below. When all values of *n* are considered, the sum of F_n values equals *P*, which, as expected corresponds to the fraction of the polymer composed of **S** subsequences in any context. This can be easily proven for any $P < 1$ by expressing the sum as a convergent geometric series:

$$\sum_1^\infty nP^n (1-P)^2 = (1-P)^2 \sum_1^\infty nP^n = (1-P)^2 \frac{P}{(1-P)^2} = P$$

The fractions F_n of the polymer composed of domains with exactly *n* tandemly repeated **S** subsequences for $P = 0.5$ and $P = 0.01$:

n	F_n (P=0.5)	F_n (P=0.01)
1	12.5%	0.98%
2	12.5%	0.02%
3	9.38%	0.00%
4	6.25%	0.00%
5	3.91%	0.00%
6	2.34%	0.00%
7	1.37%	0.00%
8	0.78%	0.00%
9	0.44%	0.00%
10	0.24%	0.00%
11	0.13%	0.00%
12	0.07%	0.00%
Total	49.91%	1.00%

A probability analysis using the abundance of XXXG subunits in the XyG from *mur3-3* (63%), *mur3-7* (73%) wild type (25%), *mur3-1* (48%), *mur3-2* (47%), and 35Spro*MUR3*:*mur3-3* (29%) plants predicts that domains consisting of 5 or more tandemly repeated XXXG sequences comprise a much higher proportion of the XyG in *mur3-3* and *mur3-7* plants than in XyG from the other plants (see Supplemental Fig. S11).